Nonlinear Spacing Policies for Automated Heavy-Duty Vehicles

Diana Yanakiev, *Member, IEEE*, and Ioannis Kanellakopoulos, *Member, IEEE*

***Abstract*—In the longitudinal control problem for automated heavy-duty vehicles, an important control objective is string stability, which ensures that errors decrease as they propagate upstream through the platoon. It is well known that when vehicles operate autonomously, string stability can be achieved by using speed-dependent spacing with constant time headway. However, this results in large steady-state intervehicle spacings, hence, decreased traffic throughput. This disadvantage is even more pronounced in heavy-duty vehicles, which require larger time headways due to their low actuation-to-weight ratio. In this paper, we develop two new *nonlinear* spacing policies—*variable time headway* and *variable separation error gain*—which all but eliminate this undesirable side effect. The first policy significantly reduces the transient errors and allows us to use much smaller spacings in autonomous platoon operation, while the second one results in smoother and more robust longitudinal control. Furthermore, the two can be combined to yield even better robustness, as is shown through our qualitative analysis.**

***Index Terms*— Autonomous operation, commercial vehicles, longitudinal control, spacing policies.**

I. Introduction

ADVANCED vehicle control system (AVCS) design is an integral part of the rapidly growing national and international initiatives on intelligent transportation systems (ITS's) and automated highway systems (AHS's), which aim at significantly increasing the traffic capacity of existing highways through vehicle and roadway automation. In the past few years, AVCS research and development has been primarily focused on passenger vehicles, while commercial heavy vehicles (CHV's) such as heavy-duty freight trucks (including tractor-trailer combinations) and commuter buses have been largely ignored. The obvious justification is that there are many more passenger vehicles on the road, and thus their automation will have the largest possible impact on the desired increase of highway traffic flow.

However, this argument does not take into account the many differences in the operational modes between commercial and passenger vehicles, which render the relative impact of CHV's on traffic congestion and economic growth much larger than their numbers suggest. In fact, the motivation for automating CHV's goes far beyond the need to include these vehicles in the automated highways of the future; it is often argued that CHV's have the potential of becoming the flagships of AHS efforts, due to several economic and policy issues.

To justify this position, let us consider one of the most visible proposed strategies for highway automation, which is to group automatically controlled vehicles in *platoons* [4]–[8], i.e., tightly spaced vehicle group formations. Since platooning is likely to improve fuel consumption, we can see why the most important reason that CHV's, and in particular heavy-duty freight trucks, are likely to be the first semiautomated or fully automated vehicles is *profit-driven operation*: the average truck travels *six times the miles* and consumes *27 times the fuel* of the average passenger car, and these numbers are even higher if restricted to heavy commercial trucks, rated at 40 000 lbs or more. Thus, even a small improvement in fuel efficiency can be incentive enough for truck fleet operators to invest in AVCS equipment. Moreover, truck traffic follows much more regular patterns than passenger car traffic; trucks usually travel on well-established commercial routes, mostly between major cities. Thus, fleet operators can easily compose platoons of trucks with the same origination and destination points which will travel together for the entire trip. Under this scenario, in the first stages of AHS deployment, freight transport companies will operate departure/arrival stations in major cities. Individual trucks will be driven manually from all over the city to the station, where they will join the platoon departing for their destination city. Each platoon will consist of several trucks, with only two drivers in the lead vehicle who can take turns driving, while the following vehicles will be driverless. In the meantime, the drivers who are not on the departing platoons will manually drive the trucks from arriving platoons to their individual points destination points within the city. This reduction in the number of drivers will yield significant savings (25% or more) in operating costs, thereby reducing the time to recovery of the initial investment and increasing the profit margin. The effect of these savings through platooning is further compounded by the fact that the ratio of intercity to intracity miles traveled by freight trucks is much higher than for passenger cars. Hence, CHV's will utilize their automation capabilities much more than passenger cars, since they spend most of their travel time on interstate highways, where they will be able to travel in platoons.

Manuscript received August 29, 1996; revised July 1, 1997. This work was supported in part by the California Department of Transportation through the California PATH Program under MOU 124 and MOU 240 and the National Science Foundation under Grants ECS-9309402 and ECS-9502945.

D. Yanakiev was with the Department of Electrical Engineering, University of California, Los Angeles, CA 90095-1594 USA. She is now with Cummins Engine Company, Inc., Columbus, IN 43210-1189 USA.

I. Kanellakopoulos is with the Department of Electrical Engineering, University of California, Los Angeles, CA 90095-1594 USA (e-mail: ioannis@ee.ucla.edu).

Publisher Item Identifier S 0018-9545(98)08141-9.

The longitudinal control problem for this type of “intercity platooning” is significantly simplified by the absence of split/merge maneuvers. However, to obtain significantly higher traffic throughput in urban freeways, platoons must operate with small intervehicle spacings and many vehicles in each group. Therefore, the longitudinal control design for platoons of automated vehicles has to guarantee the desired performance not only for each individual vehicle, but also for the whole formation. A key property is *string stability*, which ensures that errors decrease as they propagate upstream through the platoon. The fact that string stability cannot be achieved for platoons with *constant intervehicle spacing* under autonomous operation has been known for more than 20 years [3], [7]. String stability can be guaranteed if the lead vehicle is transmitting its velocity [7] or velocity and acceleration [6] to all other vehicles in the platoon. This approach yields stable platoons with small intervehicle spacings at the cost of introducing and maintaining continuous intervehicle communication with high reliability and small delays. String stability can also be recovered in autonomous operation if a *speed-dependent* spacing policy is adopted, which incorporates a *fixed time headway* term in addition to the constant distance [2], [3]. This approach avoids the communication overhead, but results in larger spacings between adjacent vehicles and, thus, in longer platoons, thereby yielding smaller increases in traffic throughput.

This problem is much more serious in the case of CHV platoons, primarily due to their low actuation-to-weight ratio: the levels of acceleration and deceleration achievable by CHV’s are almost an order of magnitude lower than for passenger cars. As we will see in Section III, this makes string stability a much more elusive goal for CHV’s; in the absence of intervehicle communication, the fixed time headway necessary for string stability is significantly larger, hence, the reduction in traffic throughput is much more pronounced. This necessitates the design of new longitudinal control algorithms, which are the focus of this paper: we design several new spacing policies and control schemes which use *nonlinearity* to endow the vehicles in the platoon with a “group conscience” and occasionally even sacrifice the individual performance of some vehicles in order to improve the performance of the whole platoon.

The remainder of the paper is organized as follows. In Section II, we formulate the control objective specific to the platoon scenario. Then we proceed with the longitudinal control design and present it in the modular framework of Section III: we start with a PI scheme based on the linearized vehicle model and develop independent “upgrades” in the subsequent sections. This format has been chosen to emphasize the fact that the modifications of the original scheme can be applied either separately or in combination. In this section, we also investigate the string stability properties of the resulting control schemes through analysis and numerical simulations of a single platoon, while in Section IV we test their robustness in a more challenging scenario involving the merger of two platoons. In the concluding Section V, we give a graphical qualitative comparison of the new control schemes, which not only summarizes the results presented in the former sections, but also allows designers to better negotiate the tradeoffs between platoon performance, control smoothness, robustness, and controller complexity in the choice of a scheme which best fits the needs of a particular implementation.

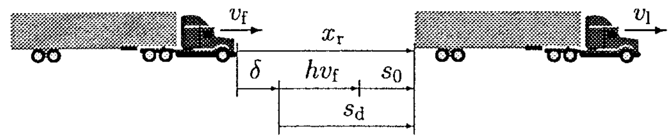

s_0 : minimum distance between vehicles
h : time headway
x_{r} : vehicle separation
$s_{\mathrm{d}} = s_0 + hv_{\mathrm{f}}$: desired vehicle separation
v_{l} : velocity of leading vehicle
v_{f} : velocity of following vehicle
$v_{\mathrm{r}} = v_{\mathrm{l}} - v_{\mathrm{f}}$: relative vehicle velocity
$\delta = x_{\mathrm{r}} - s_{\mathrm{d}}$: separation error

Fig. 1. Parameters of a truck platoon.

II. Control Objective

The parameters relevant to any two adjacent vehicles in a platoon are illustrated in Fig. 1.

In the platoon scenario, the controller has to regulate to zero both the relative velocity v_r and the separation error δ

$$v_r = v_{\mathrm{l}} - v_f \quad \delta = x_r - s_d \tag{1}$$

where v_{l} and v_f are the velocities of the leading and following vehicles, while x_r is the actual and s_d the desired separation between vehicles. The desired separation may be constant (fixed spacing policy) or a function of the follower’s velocity

$$s_d = s_0 + hv_f \tag{2}$$

as shown in Fig. 1. The parameter h is called *time headway*, and its effect is to introduce more spacing at higher velocity in addition to the *constant spacing* s_0. An alternative way to introduce speed-dependent spacing would be to make it a function of the leader’s velocity, i.e., $s_d = s_0 + hv_{\mathrm{l}}$. However, this strategy has a fundamental flaw: if the follower travels at a much higher speed than the leader, say 70 versus 40 mph, the desired spacing would be based on the leader’s lower speed; this significantly increases the likelihood of severe collisions. The tasks of regulating the relative velocity and the separation error can be combined into the control objective $v_r + k\delta = 0$, where k is a positive design constant. This control objective makes sense intuitively: if two vehicles are closer than desired ($\delta < 0$) and the control objective is satisfied ($v_r = -k\delta > 0$), then the follower is moving slower than the leader, which is exactly what one wants. The same can be said if the vehicles are farther apart than desired ($\delta > 0$), in which case $v_r = -k\delta < 0$ means that the follower’s speed is higher than the leader’s. The selection of the coefficient k influences the response of the controller and can be changed depending on the performance requirements. In fact, as we will see beginning with Section III-E, making this coefficient a nonlinear function of the separation error δ can significantly enhance platoon performance as well as control smoothness.

Let us now show that when our control objective is achieved, i.e., when $v_r+k\delta \equiv 0$, both the relative velocity and the separation error are regulated: $v_r \to 0$ and $\delta \to 0$. When the velocity of the lead vehicle is constant ($\dot{v}_1 = 0$), we have

$$\delta = x_r - s_d = x_r - hv_f - s_0 \Rightarrow \dot{\delta} = v_r - h\dot{v}_f \tag{3}$$

$$v_r = v_1 - v_f \Rightarrow \dot{v}_r = -\dot{v}_f. \tag{4}$$

But $v_r + k\delta \equiv 0$ implies that

$$\dot{v}_r + k\dot{\delta} \equiv 0. \tag{5}$$

Combining this with (3) and (4), we obtain

$$\dot{v}_r + k(v_r + h\dot{v}_r) \equiv 0 \Rightarrow (1+kh)\dot{v}_r + kv_r \equiv 0 \tag{6}$$

which shows that $v_r \to 0$ (since $k > 0$ and $h > 0$). From $v_r + k\delta \equiv 0$ and $v_r \to 0$ we conclude that $\delta \to 0$.

In general, for variables h or k, the above is not necessarily true and has to be shown for the particular form of h or k, respectively.

III. Control Design

Most of the available results on longitudinal control of automated vehicles use separate controllers for the fuel and the brake with some *ad hoc* logic for switching from one to the other. In contrast, our controllers activate both; this is suggested by the fact that the fuel and the brake command are mutually exclusive in nature. This approach is appealing because it eliminates the undesirable overhead associated with switching between controllers, thus providing a less complicated and more reliable design. When the output of the controller is positive, a fuel command is issued, while a negative output activates the brakes. In order to avoid excessive switching between fuel and brake command in the region around zero, a hysteresis element is added to the controller output.

Following [12], we use a first-order-linearized vehicle model as the starting point for the design of our longitudinal control schemes; in our simulations, however, we always use the full nonlinear vehicle model described in [12], comprising eight states and numerous nonlinearities. Since the control objective is to maintain $v_r + k\delta = 0$, we linearize the nonlinear model around the corresponding trajectory and obtain

$$\dot{v}_f = a(v_r + k\delta) + bu + d \tag{7}$$

where the term d incorporates external disturbances as well as modeling errors.

To illustrate the various features of our control design framework, we use simulations of a platoon comprising ten tractor–semitrailer combination vehicles. Each vehicle weighs 20 000 kg (44 000 lbs) and is powered by a 14-l turbocharged diesel engine capable of producing approximately 1000 Nm (740 ft–lbs) in peak torque and 300 kW (400 hp) in peak power. The platoon starts out at an initial speed of 22 m/s (49.10 mph). At $t = 10$ s, the platoon leader decides to reduce his speed by 10 m/s (22.32 mph) and then, at $t =$ 80 s, to increase it by 5 m/s (11.16 mph). The minimum desired separation between vehicles is $s_0 = 3$ m. This demanding scenario is representative of the difficulties the system might have maintaining string stability when trying to meet a challenging acceleration/deceleration objective. In all our simulation plots, different vehicles are represented by lines of different styles: Vehicle 1 is shown with a solid line, while following vehicles cycle through dash–dotted, dashed, dotted, and solid lines (so that, for example, Vehicles 5 and 9 are shown with solid lines).

A. PI Controller

Since our simplified longitudinal model is a first-order linear system, the proportional integral (PI) controller is the simplest controller which can achieve regulation of both v_r and δ with some robustness with respect to disturbances and unmodeled effects. Hence, the PI controller is the starting point of our control design. The control law is

$$u = k_p(v_r + k\delta) + k_i\frac{1}{s}(v_r + k\delta) \tag{8}$$

where k_p is the proportional and k_i is the integral gain.

However, in the demanding scenario of the presented simulations, a simple PI controller is not adequate. Therefore, we introduce several modifications in order to improve platoon performance and smoothness of control effort. These modifications of the control law can be viewed as independent modules which may be used separately or combined. By qualitatively evaluating the contribution of each module, we can add complexity to the control design only as needed to meet the given performance specifications.

B. Signed Quadratic (Q) Term

The lower actuation-to-weight ratio of heavy-duty vehicles requires a controller which is more aggressive at large errors, but does not have the undesirable side effect of overshoot. This is achieved by adding a signed quadratic (Q) term of the form $(v_r + k\delta)|v_r + k\delta|$ to the PI controller, which thus becomes a nonlinear PIQ controller

$$u = k_p(v_r + k\delta) + k_i\frac{1}{s}(v_r + k\delta) + k_{\mathrm{q}}(v_r + k\delta)|v_r + k\delta|. \tag{9}$$

This Q term was used successfully in the speed control problem of heavy-duty vehicles in [12], where it proved to be more efficient in avoiding overshoot than an antiwindup term and provided faster attenuation of errors compared to linear controllers. It also performed well in the platoon scenario, where overshoot is even less desirable.

C. Adaptive Gains

Even if a controller is perfectly tuned for some operating region, it is likely to demonstrate inferior performance in other conditions due to the severe nonlinearities present in the system. A gain scheduling approach could be successful in overcoming the disadvantages of a fixed gain controller, but it would require extensive *a priori* information. Moreover, due to large variations in the mass of heavy-duty vehicles (the change in mass between a lightly and heavily loaded truck can be as much as 300%), such *a priori* information may even be impossible to obtain. Adaptation of the control gains is the natural solution, since it makes the closed-loop system response much less dependent on the current operating region and on the specific vehicle characteristics. The latter consideration becomes more significant in the platoon scenario where even if the grouped vehicles are not identical, they are expected to respond uniformly to different commands or disturbances.

The adaptive PI control law is

$$u = \hat{k}_p(v_r + k\delta) + \hat{k}_i \tag{10}$$

and the adaptive PIQ is

$$u = \hat{k}_p(v_r + k\delta) + \hat{k}_i + \hat{k}_{\mathrm{q}}(v_r + k\delta)|v_r + k\delta| \tag{11}$$

where $\hat{k}_p$, $\hat{k}_i$, and $\hat{k}_{\mathrm{q}}$ are time-varying parameters which are being updated by an adaptive law. We are going to derive the parameter update laws only for the adaptive PIQ controller, and then show the modification necessary to obtain the adaptive PI control law.

Substituting (11) into (7) yields

$$\dot{v}_f = (a + b\hat{k}_p)(v_r + k\delta) + b\hat{k}_i + b\hat{k}_{\mathrm{q}}\ (v_r + k\delta)\ |v_r + k\delta| + \bar{d}. \tag{12}$$

To design update laws for the parameter estimates, we consider a nonlinear reference model

$$\dot{v}_{\mathrm{m}} = a_{\mathrm{m}}(v_{\mathrm{l}} - v_{\mathrm{m}} + k\delta) + q_{\mathrm{m}}(v_{\mathrm{l}} - v_{\mathrm{m}} + k\delta)|v_r + k\delta| \tag{13}$$

where $a_{\mathrm{m}} > 0$ and $q_{\mathrm{m}} \geq 0$. If a, b, and d were known, the coefficients of the controller could be chosen so that the plant and the reference model would respond identically to the same input signal. The corresponding values k_p, k_i, and k_{q} are computed from the following:

$$\begin{aligned} a + bk_p &= a_{\mathrm{m}} \\ bk_i &= -d \\ bk_{\mathrm{q}} &= q_{\mathrm{m}}. \end{aligned} \tag{14}$$

Since the parameters of the plant are unknown, we replace k_p, k_i, and k_{q} by their estimates in the control law (11). To design update laws for these estimates, we use the tracking error $e_r = v_f - v_{\mathrm{m}}$ computed from (12) to (14) as

$$\begin{aligned} \dot{e}_r &= \dot{v}_f - \dot{v}_{\mathrm{m}} \\ &= -a_{\mathrm{m}}e_r - q_{\mathrm{m}}e_r|v_r + k\delta| \\ &\quad - b[\tilde{k}_p(v_r + k\delta) + \tilde{k}_i + \tilde{k}_{\mathrm{q}}(v_r + k\delta)|v_r + k\delta|]. \end{aligned} \tag{15}$$

where $\tilde{k}_p = k_p - \hat{k}_p$, $\tilde{k}_i = k_i - \hat{k}_i$, and $\tilde{k}_{\mathrm{q}} = k_{\mathrm{q}} - \hat{k}_{\mathrm{q}}$ are the parameter errors.

Then, the update law may be obtained via the complete Lyapunov function of our closed-loop system [12]. Here, we use a simplified design which works just as well; we obtain the update law via the partial Lyapunov function[1]

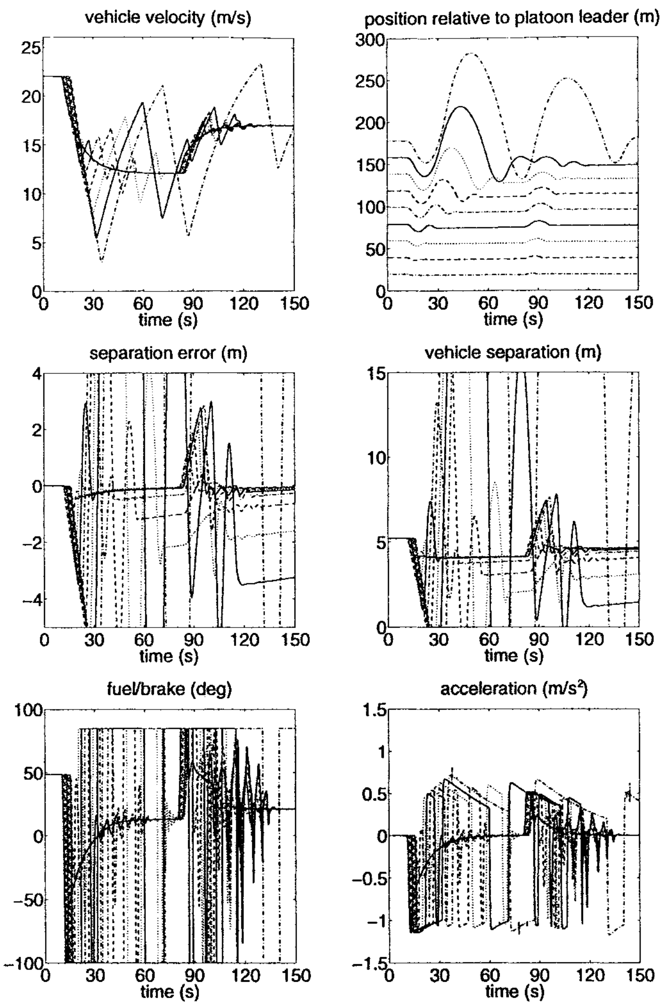

Fig. 2. Ten autonomous vehicles, constant $h = 0.1$ s.

$$V = \frac{e_r^2}{2} + b\frac{\tilde{k}_p^2}{2\gamma_p} + b\frac{\tilde{k}_i^2}{2\gamma_i} + b\frac{\tilde{k}_{\mathrm{q}}^2}{2\gamma_{\mathrm{q}}} \tag{16}$$

where γ_p, γ_i, and γ_{q} are positive design constants and b is unknown, but positive. With the choices

$$\begin{aligned} \dot{\hat{k}}_p &= \mathrm{Proj}[-\gamma_p e_r(v_r + k\delta)] \\ \dot{\hat{k}}_i &= \mathrm{Proj}[-\gamma_i e_r] \\ \dot{\hat{k}}_{\mathrm{q}} &= \mathrm{Proj}[-\gamma_{\mathrm{q}} e_r(v_r + k\delta)|v_r + k\delta|] \end{aligned} \tag{17}$$

where $\mathrm{Proj}[\cdot]$ is the projection operator to a compact interval containing the true value of the parameter, we obtain for $\dot{V}$

$$\dot{V} = -a_{\mathrm{m}}e_r^2 - q_{\mathrm{m}}|v_r + k\delta|e_r^2 \leq 0. \tag{18}$$

This guarantees the boundedness of e_r, $\hat{k}_1$, $\hat{k}_2$, and $\hat{k}_3$ and the regulation of e_r.

The derivation of the parameter update laws for the adaptive PI controller is obtained by setting $q_{\mathrm{m}} = 0$ in the reference

[1] This Lyapunov function is called partial because it does not include the states v_r and δ which are part of our controller dynamics.

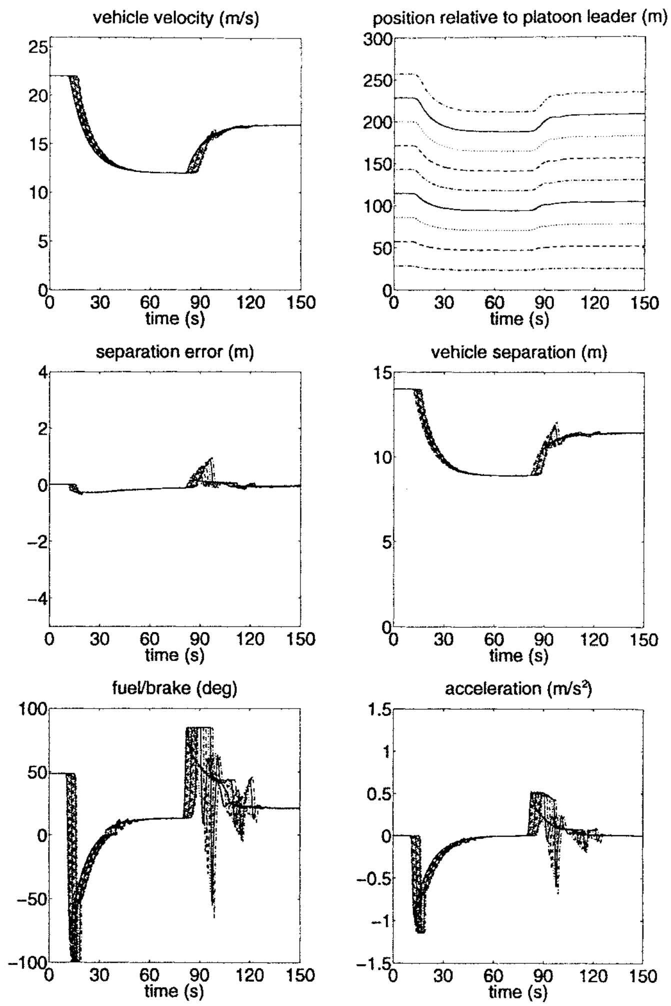

Fig. 3. Ten autonomous vehicles, constant $h = 0.5$ s.

model (13) which yields the same update laws for $\hat{k}_p$ and $\hat{k}_i$. From (17) we see that the $\hat{k}_i$ term in (10) and (11) is indeed an "integral" term, since it is the integral of the error e_r. This term attenuates the effects of external disturbances such as road grades and headwinds, and it also provides the nominal control value necessary to maintain a constant speed with zero steady-state error.

The resulting adaptive PIQ controller can operate autonomously using a speed-dependent spacing policy. However, the fixed time headway has to be significantly larger than for passenger cars in order to guarantee good CHV platoon performance. This is illustrated in Fig. 2, which shows that with time headway $h = 0.1$ s the errors are significantly amplified as they propagate upstream through the platoon (from Vehicle 1 to Vehicle 10). As can be seen from the "vehicle separation" plot, there are even several collisions between Vehicles 7–9 (a collision is indicated by a "vehicle separation" curve which becomes negative). In order to get acceptable performance and avoid collisions, one must increase the headway to $h = 0.5$ s. Then, as seen in Fig. 3, errors become much smaller and the fuel/brake activity much smoother (implying better fuel efficiency), but the intervehicle spacing grows significantly from about 4–5 to 10–14 m. The value of 0.5 s for the constant time headway is substantially larger than the 0.1–0.2 s which yields good results for passenger cars. This increase is mainly due to the typically five–ten times smaller actuation-to-weight ratio of CHV's. It is worth noting that even larger time headway ($h \approx 1$ s) would be necessary here to guarantee string stability, i.e., attenuation of errors upstream through the platoon.

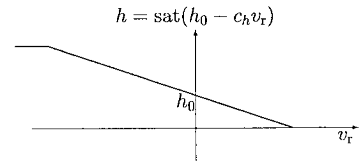

Fig. 4. Variable time headway $h = \mathrm{sat}(h_0 - c_h v_r)$.

D. Variable Time Headway (Variable h)

Intervehicle communication may not be implemented in the beginning stages of truck automation, and even if it is implemented, it may sometimes fail. Therefore, it is desirable to develop control algorithms which yield small separation errors without increased intervehicle spacing under autonomous vehicle operation. Such algorithms could be used not only under autonomous operation, but also in the intervehicle communication scenario as "backups" for the case of communication malfunctions or even failures. For the rest of this paper, we will focus on the development of new nonlinear spacing policies which achieve this goal.

First, we introduce the notion of *variable time headway*, i.e., a headway which instead of being constant varies with the relative speed v_r between adjacent vehicles. The intuition behind this modification, which was first presented in [11], is as follows: suppose that a vehicle wants to maintain a 0.1-s time headway from the preceding vehicle, when both of them are traveling at the same speed. If the relative speed between the two vehicles is positive, that is, if the preceding vehicle is moving faster, then it is safe to reduce this headway, while if the preceding vehicle is moving slower, then it would be advisable to increase the headway. This leads to the following choice for h as a function of the relative velocity v_r:

$$h = h_0 - c_h v_r \tag{19}$$

where $h_0 > 0$ and $c_h > 0$ are constant. For safety reasons, the headway h cannot be allowed to become negative, while very large headways are undesirable as shown in [12]. Thus, we limit the headway in the interval [0, 1] and arrive at the form of h shown in Fig. 4

$$h = \mathrm{sat}(h_0 - c_h v_r) = \begin{cases} 1, & \text{if } h_0 - c_h v_r \geq 1 \\ h_0 - c_h v_r, & \text{if } 0 < h_0 - c_h v_r < 1 \\ 0, & \text{otherwise.} \end{cases} \tag{20}$$

The effect of introducing the variable time headway $h = \mathrm{sat}(0.1 - 0.2 v_r)$ in our ten-truck platoon is quite dramatic, as seen in Fig. 5. Comparing Fig. 5 with Fig. 2 reveals an impressive reduction of errors and a considerably smoother control activity without any increase in steady-state intervehicle spacing. In fact, the response is quite similar to that

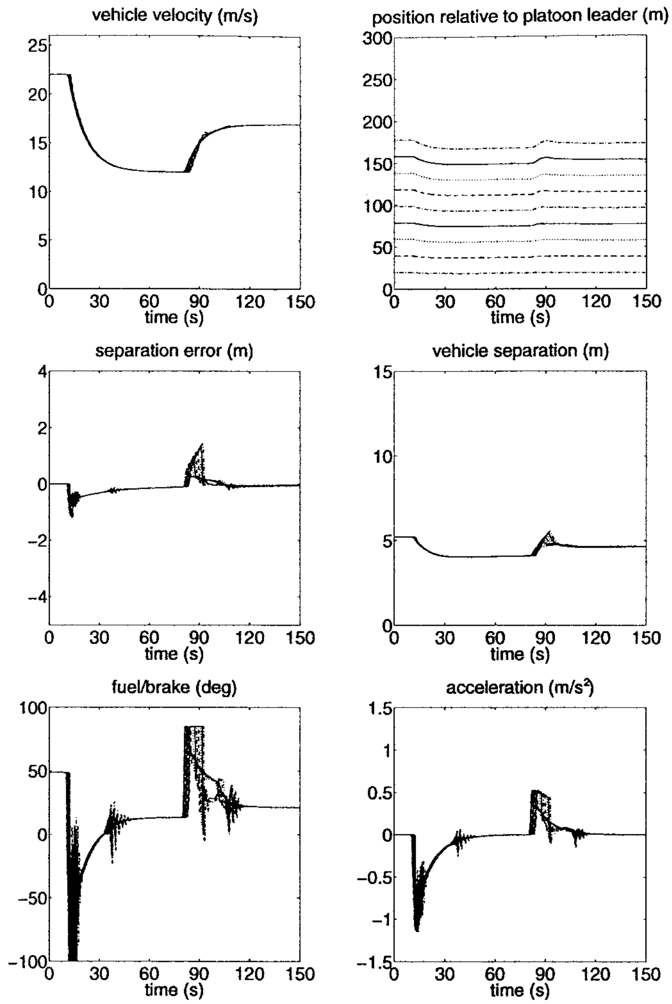

Fig. 5. Ten autonomous vehicles, $h = \mathrm{sat}(0.1 - 0.2v_r)$.

obtained with $h = 0.5$ s in Fig. 3, but with much smaller intervehicle spacing.

E. Variable Separation Error Gain (Variable k)

Another simple modification is the introduction of a *variable separation error gain* k. Recall that the intuition behind choosing the control objective as regulation of $v_r + k\delta$ was as follows: if two vehicles are closer than desired ($\delta < 0$) but the preceding vehicle's speed is larger than the follower's ($v_r > 0$), then the controller in the following vehicle does not need to take drastic action, and the same is true if the vehicles are farther apart than desired ($\delta > 0$), but the preceding vehicle's speed is lower than the follower's ($v_r < 0$). However, when the separation error gain k is constant, the controller will try to reduce a very large spacing error δ through a very large relative velocity v_r of opposite sign. Hence, if a vehicle falls far behind the preceding vehicle, its controller will react aggressively by accelerating to a very high speed. This behavior is not only undesirable, since it increases fuel consumption and can even lead to collisions in extreme situations, but is also counter-intuitive. It would be much more natural for the controller to accelerate to a speed somewhat higher than that of the preceding vehicle's and reduce the spacing error smoothly and progressively. To achieve such a response, we need to decrease the gain k as δ becomes large and positive, making sure that it remains above some reasonable positive lower bound. The choice of k

$$k = c_k + (k_0 - c_k)e^{-\sigma\delta^2} \tag{21}$$

where $0 < c_k < k_0$ and $\sigma \geq 0$ are design constants, satisfies this requirement. This choice of k, shown in Fig. 6, makes the control objective $v_r + k\delta = 0$ nonlinear in δ. It also has another feature which at first glance may seem counter-intuitive: the gain k is reduced even when δ becomes negative. A careful examination of the truck platoon characteristics and of the simulation results yields the following explanation for this choice: in autonomous operation, each vehicle relies only on its own measurements of relative speed and distance from the preceding vehicle. This means that if the preceding vehicle suddenly decelerates, then the following vehicle will have to decelerate even more to maintain the desired spacing. Hence, to maintain string stability, aggressive control actions must be amplified as they propagate upstream through the platoon. While this may not be a big problem for passenger cars, it becomes crucial for CHV's due to their low actuation-to-weight ratio which severely limits the accelerations and decelerations they are capable of achieving. During a sudden braking maneuver, only the first few vehicles in the platoon will be able to achieve the necessary decelerations; the controllers of the next vehicles will quickly saturate, and collisions may occur. In fact, the likelihood of a collision increases with the number of vehicles in the platoon. On the other hand, if the reaction of the first few vehicles is not as aggressive, then the decelerations are not amplified as much, and, hence, the remaining vehicles can achieve the necessary profiles. In a sense, reducing the gain k for negative δ endows the controller with a "platoon conscience," which sacrifices the individual performance of the first few vehicles in order to improve the overall behavior of the platoon. This is clearly illustrated in Fig. 7, which uses $k_0 = 1$, $c_k = 0.1$, and the same fixed headway $h = 0.1$ s as Fig. 2. Comparing the two figures, we see that the use of variable k yields significantly improved platoon performance: the errors are not amplified as they propagate upstream through the platoon, there are no collisions, and the control effort is noticeably smoother. However, the errors of the first five vehicles are larger than in Fig. 2 because their controllers did not react as aggressively. The individual performance of these vehicles has been compromised, but the improvement in the performance of the remaining vehicles results in a better overall tradeoff.

F. Variable h and Variable k

As mentioned previously, the "modules" described so far in this section can be used in the controller separately or in combination. Hence, we now set out to examine the asymptotic convergence and string stability properties of the resulting closed-loop system, in the case where both k and h are variable.

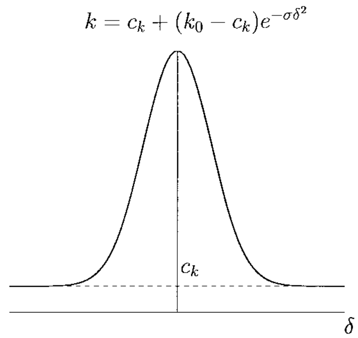

Fig. 6. Variable k choice.

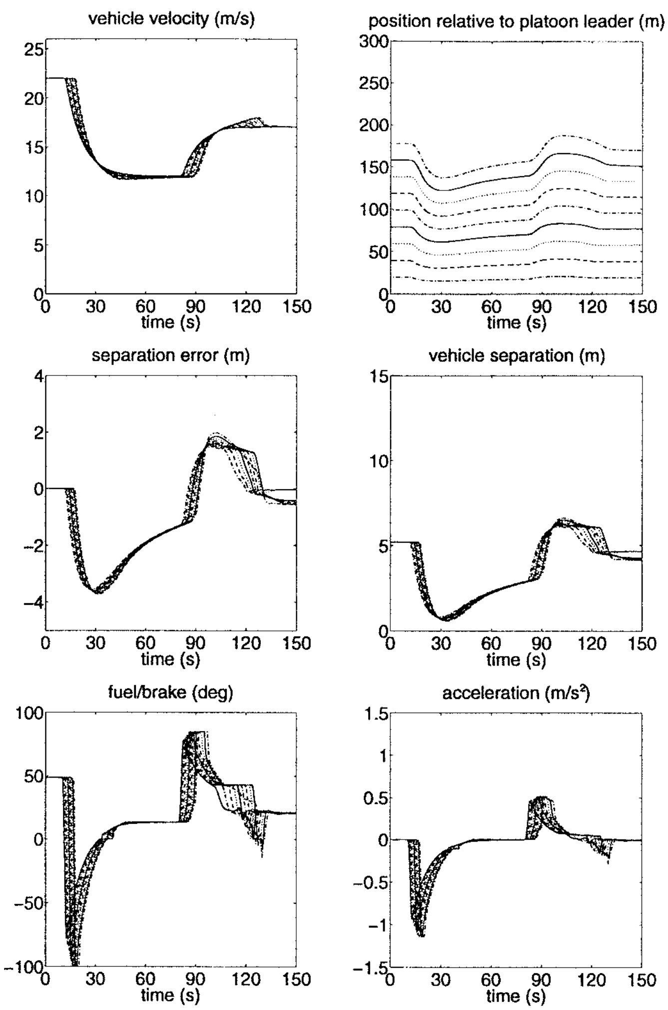

Fig. 7. Ten autonomous vehicles, $h = 0.1$ s, variable k, $\sigma = 50$.

1) Asymptotic Convergence: First, we need to verify that when the control objective $v_r + k\delta \equiv 0$ is achieved, both the relative velocity v_r and the separation error δ converge to zero. When $v_r + k\delta \equiv 0$, we have

$$\dot{v}_r + \dot{k}\delta + k\dot{\delta} \equiv 0. \tag{22}$$

For variable h, (3) becomes

$$\delta = x_r - hv_f - s_0 \Rightarrow \dot{\delta} = v_r - h\dot{v}_f - \dot{h}v_f. \tag{23}$$

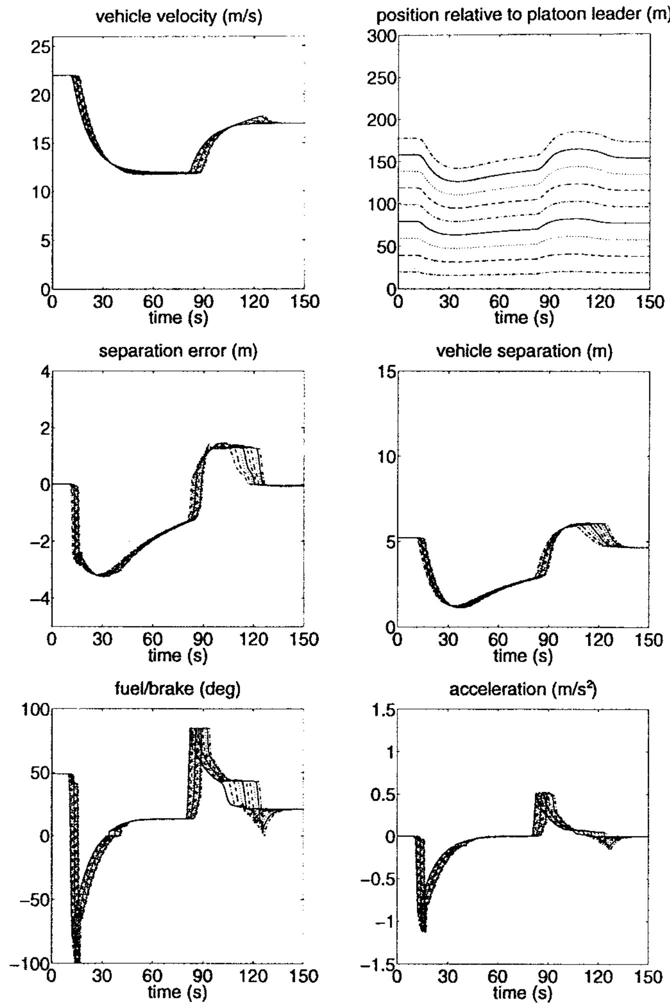

Fig. 8. Ten autonomous vehicles, $h = \mathrm{sat}(0.1 - 0.2v_r)$, variable k, $\sigma = 50$.

Combining this with (4), (20), and (22), we obtain

$$\dot{\delta} = -k\delta + (h + \alpha(h)c_h v_f)\Big(-k\dot{\delta} - \dot{k}\delta\Big) \tag{24}$$

$$\alpha(h) = \begin{cases} 1, & 0 < h < 1 \\ 0, & \text{otherwise.} \end{cases}$$

With our particular choice of k, given in (21), this expression becomes

$$\dot{\delta}\Big\{1 + (h + \alpha(h)c_h v_f)\Big[c_k + (k_0 - c_k)e^{-\sigma\delta^2}\big(1 - 2\sigma\delta^2\big)\Big]\Big\} + k\delta \equiv 0. \tag{25}$$

The term in the square brackets

$$\phi(\delta) = c_k + (k_0 - c_k)e^{-\sigma\delta^2}\big(1 - 2\sigma\delta^2\big)$$

achieves its minimum value of $c_k - 2(k_0 - c_k)e^{-3/2}$ at $\delta = \pm\sqrt{3/2\sigma}$. Therefore, the condition

$$h < \frac{1}{2(k_0 - c_k)e^{-3/2} - c_k} \tag{26}$$

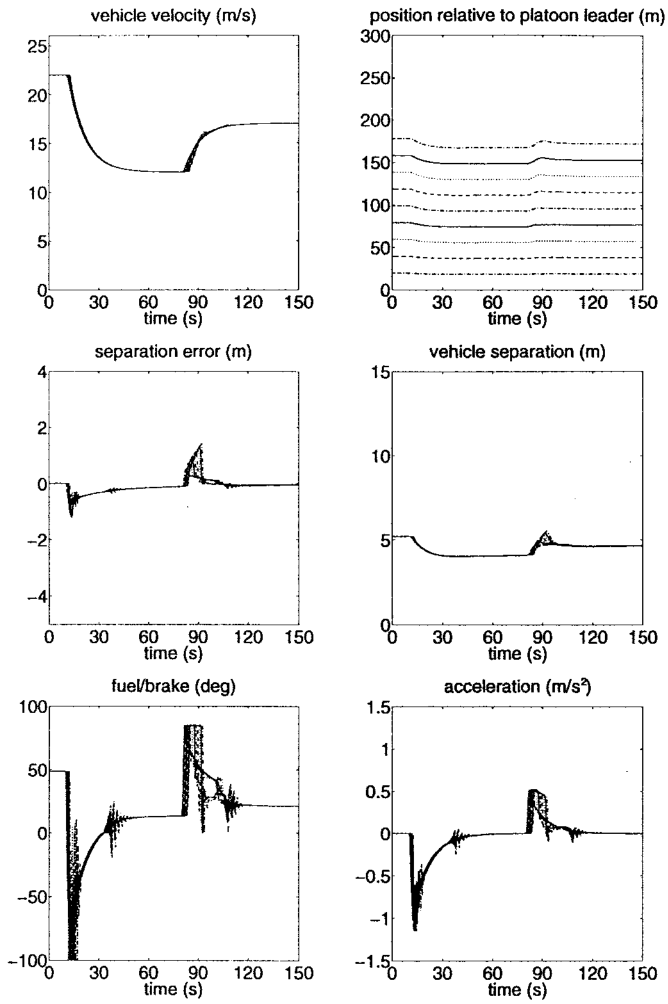

Fig. 9. Ten autonomous vehicles, $h = \mathrm{sat}(0.1 - 0.2v_r)$, variable k, $\sigma = 0.1$.

gives $1 + h\phi(\delta) > 0$ and (since $v_f > 0$) $1 + (h + \alpha(h)c_h v_f)\phi(\delta) > 0$ for all values of δ. Combined with (25) and the boundedness of v_f and $\phi(\delta)$, this guarantees that $\delta \to 0$. From $v_r + k\delta \equiv 0$ and $\delta \to 0$, we conclude that $v_r \to 0$. We have to note that the condition (26) is a conservative one since it is computed using the worst case value $\delta = \pm\sqrt{3/2\sigma}$. Thus, it is sufficient, but not necessary for the convergence of δ to zero. Nevertheless, this condition is automatically satisfied with our choices: substituting $k_0 = 1$ and $c_k = 0.1$ into (26) yields the condition $h < 3.3$, while (20) guarantees that our variable h satisfies $0 \leq h \leq 1$.

Simulation results for the case when both the time headway and the vehicle separation gain are variable are shown in Figs. 8 and 9. Comparing these two figures with Figs. 5 and 7, we see that the value of the constant σ determines whether the variable separation error gain or the variable time headway is the dominating factor in dictating platoon performance. For large values of σ, the variable k dominates; the response in Fig. 8, where $\sigma = 50$ is used, is very similar to that in Fig. 7. On the other hand, for small σ, it is the variable h that takes precedence; Fig. 9, with $\sigma = 0.1$, is almost identical to Fig. 5.

2) String Stability: One way to investigate string stability, i.e., to see how the separation errors propagate upstream through the platoon, is to consider the transfer function $G(s) = \delta_i(s)/\delta_{i-1}(s)$, where i is the vehicle number in the platoon. The requirement for upstream attenuation of errors will be satisfied when

$$|G(j\omega)| = \left|\frac{\delta_i(j\omega)}{\delta_{i-1}(j\omega)}\right| < 1, \qquad \forall\, \omega > 0. \tag{27}$$

Even though transfer function analysis does not take into account the effect of the initial conditions, it provides considerable insight and a firm basis for comparison between the different spacing policies. We emphasize that (27) is necessary, but not sufficient for string stability: it is not sufficient because it is based on linearization analysis and, hence, will not apply to large errors resulting from challenging maneuvers. However, since our controllers are supposed to keep the errors small, this analysis is useful for many practical cases. On the other hand, it is necessary: if $|G(j\omega_0)| > 1$ for some frequency ω_0, one can generate errors that increase upstream by using a small sinusoidal reference input of frequency ω_0 for the platoon leader.

The adaptation of the controller parameters is assumed to be fast enough so that v_i can be approximated by v_{m}: $e_r \to 0$ for constant v_{i-1}. Then, setting $q_{\mathrm{m}} = 0$ in (13) to obtain a PI controller, we have

$$\dot{v}_i = a_{\mathrm{m}}(v_{r,\,i} + k_i\delta_i) \tag{28}$$

and

$$\begin{aligned}\dot{v}_{r,\,i} &= \dot{v}_{i-1} - \dot{v}_i \\ &= a_{\mathrm{m}}(v_{r,\,i-1} + k_{i-1}\delta_{i-1}) - a_{\mathrm{m}}(v_{r,\,i} + k_i\delta_i).\end{aligned} \tag{29}$$

Recall that $\delta_i = x_{r,\,i} - h_i v_i - s_0$, where h_i denotes the current value of the variable time headway used by vehicle i. Using (20) for the choice of variable h and assuming small enough variations to avoid the saturation regions of h, we obtain

$$\begin{aligned}\dot{\delta}_i &= v_{r,\,i} - h_i\dot{v}_i - \dot{h}_i v_i \\ &= v_{r,\,i} - h_0\dot{v}_i + c_h\dot{v}_{r,\,i}v_i + c_h v_{r,\,i}\dot{v}_i\end{aligned} \tag{30}$$

or

$$v_{r,\,i} = \dot{\delta}_i + h_0\dot{v}_i - c_h\dot{v}_{r,\,i}v_i - c_h v_{r,\,i}\dot{v}_i. \tag{31}$$

Differentiation of (30) yields

$$\begin{aligned}\ddot{\delta}_i &= \dot{v}_{r,\,i} - h_0\ddot{v}_i + c_h\ddot{v}_{r,\,i}v_i + 2c_h\dot{v}_{r,\,i}\dot{v}_i + c_h v_{r,\,i}\ddot{v}_i \\ &= a_{\mathrm{m}}(v_{r,\,i-1} + k_{i-1}\delta_{i-1} - v_{r,\,i} - k_i\delta_i) \\ &\quad - h_0 a_{\mathrm{m}}\Big(\dot{v}_{r,\,i} + k_i\dot{\delta}_i + \dot{k}_i\delta_i\Big) + c_h a_{\mathrm{m}} \\ &\quad \cdot \Big(\dot{v}_{r,\,i-1} + k_{i-1}\dot{\delta}_{i-1} + \dot{k}_{i-1}\delta_{i-1} - \dot{v}_{r,\,i} - k_i\dot{\delta}_i - \dot{k}_i\delta_i\Big) \\ &\quad \cdot v_i + c_h a_{\mathrm{m}}\Big(2\dot{v}_{r,\,i}v_{r,\,i} + 2\dot{v}_{r,\,i}k_i\delta_i + v_{r,\,i}\dot{v}_{r,\,i} \\ &\qquad + v_{r,\,i}k_i\dot{\delta}_i + v_{r,\,i}\dot{k}_i\delta_i\Big).\end{aligned} \tag{32}$$

Using (31) twice, first with i replaced by $i-1$ and then with i, to expand the first term in (32), results in

$$\begin{aligned}\ddot{\delta}_i =& a_{\rm m}\Big(\dot{\delta}_{i-1}+h_0\dot{v}_{i-1}-c_h\dot{v}_{r,i-1}v_{i-1}-c_hv_{r,i-1}\dot{v}_{i-1}\\ &+k_{i-1}\delta_{i-1}-\dot{\delta}_i-h_0\dot{v}_i+c_h\dot{v}_{r,i}v_i+c_hv_{r,i}\dot{v}_i-k_i\delta_i\Big)\\ &-h_0a_{\rm m}(\dot{v}_{i-1}-\dot{v}_i)-h_0a_{\rm m}\Big(k_i\dot{\delta}_i+\dot{k}_i\delta_i\Big)\\ &+c_ha_{\rm m}(\dot{v}_{r,i-1}-\dot{v}_{r,i})v_i+c_ha_{\rm m}\\ &\cdot\Big(k_{i-1}\dot{\delta}_{i-1}+\dot{k}_{i-1}\delta_{i-1}-k_i\dot{\delta}_i-\dot{k}_i\delta_i\Big)\\ &\cdot(v_{i-1}-v_{r,i})+c_ha_{\rm m}\\ &\cdot\Big(3\dot{v}_{r,i}v_{r,i}+2\dot{v}_{r,i}k_i\delta_i+v_{r,i}k_i\dot{\delta}_i+v_{r,i}\dot{k}_i\delta_i\Big)\\ =& a_{\rm m}\dot{\delta}_{i-1}+a_{\rm m}k_{i-1}\delta_{i-1}-a_{\rm m}(1+h_0k_i)\dot{\delta}_i-a_{\rm m}k_i\delta_i\\ &+c_ha_{\rm m}k_{i-1}\dot{\delta}_{i-1}v_{i-1}-c_ha_{\rm m}k_i\dot{\delta}_iv_{i-1}-c_ha_{\rm m}\dot{v}_{r,i-1}v_{r,i}\\ &-c_ha_{\rm m}v_{r,i-1}\dot{v}_{r,i}+c_ha_{\rm m}v_{r,i}\dot{v}_i-c_ha_{\rm m}k_{i-1}\dot{\delta}_{i-1}v_{r,i}\\ &+c_ha_{\rm m}k_i\dot{\delta}_iv_{r,i}+c_ha_{\rm m}\dot{v}_{r,i}(3v_{r,i}+2k_i\delta_i)\\ &+c_ha_{\rm m}v_{r,i}k_i\dot{\delta}_i-a_{\rm m}[h_0+c_h(v_i-v_{r,i})]\dot{k}_i\delta_i\\ &+c_ha_{\rm m}\dot{k}_{i-1}\delta_{i-1}v_i. \end{aligned} \quad (33)$$

For our choice of k, we denote

$$\dot{k}=-2\sigma\delta(k_0-c_k)e^{-\sigma\delta^2}\dot{\delta}\triangleq\psi(\delta)\delta\dot{\delta}. \quad (34)$$

Substitution of (28)–(30) and (34) into (33) results in

$$\begin{aligned}\ddot{\delta}_i =& a_{\rm m}(1+c_hk_{i-1}v_{i-1})\dot{\delta}_{i-1}+a_{\rm m}k_{i-1}\delta_{i-1}\\ &-a_{\rm m}(1+h_0k_i+c_hk_iv_{i-1})\dot{\delta}_i-a_{\rm m}k_i\delta_i\\ &+c_ha_{\rm m}^2(v_{r,i-2}+k_{i-2}\delta_{i-2}-v_{r,i-1}-k_{i-1}\delta_{i-1})v_{r,i}\\ &-c_ha_{\rm m}^2v_{r,i-1}(v_{r,i-1}+k_{i-1}\delta_{i-1})\\ &+c_ha_{\rm m}^2v_{r,i}(v_{r,i}+k_{i-1}\delta_i)-c_ha_{\rm m}k_{i-1}v_{r,i}\\ &\cdot[v_{r,i-1}-h_0a_{\rm m}(v_{r,i-1}+k_{i-1}\delta_{i-1})\\ &+c_ha_{\rm m}(v_{r,i-2}+k_{i-2}\delta_{i-2}-v_{r,i-1}-k_{i-1}\delta_{i-1})\\ &\cdot v_{i-1}+c_ha_{\rm m}v_{r,i-1}(v_{r,i-1}+k_{i-1}\delta_{i-1})]\\ &+2c_ha_{\rm m}k_iv_{r,i}[v_{r,i}-h_0a_{\rm m}(v_{r,i}+k_i\delta_i)\\ &+c_ha_{\rm m}(v_{r,i-1}+k_{i-1}\delta_{i-1}-v_{r,i}-k_i\delta_i)v_i\\ &+c_ha_{\rm m}v_{r,i}(v_{r,i}+k_i\delta_i)]+c_ha_{\rm m}^2\\ &\cdot(v_{r,i-1}+k_{i-1}\delta_{i-1}-v_{r,i}-k_i\delta_i)(3v_{r,i}+2k_i\delta_i)\\ &-a_{\rm m}[h_0+c_h(v_i-v_{r,i})]\psi(\delta_i)\delta_i^2\\ &\cdot[v_{r,i}-h_0a_{\rm m}(v_{r,i}+k_i\delta_i)\\ &+c_ha_{\rm m}(v_{r,i-1}+k_{i-1}\delta_{i-1}-v_{r,i}-k_i\delta_i)v_i\\ &+c_ha_{\rm m}v_{r,i}(v_{r,i}+k_i\delta_i)]+c_ha_{\rm m}v_i\psi(\delta_{i-1})\delta_{i-1}^2\\ &\cdot[v_{r,i-1}-h_0a_{\rm m}(v_{r,i-1}+k_i\delta_{i-1})\\ &+c_ha_{\rm m}(v_{r,i-2}+k_{i-2}\delta_{i-2}-v_{r,i-1}-k_{i-1}\delta_{i-1})\\ &\cdot v_{i-1}+c_ha_{\rm m}v_{r,i-1}(v_{r,i-1}+k_{i-1}\delta_{i-1})]. \end{aligned} \quad (35)$$

Linearizing (35) around $v_r=0$ and $\delta=0$ yields

$$\begin{aligned}&\ddot{\delta}_i+a_{\rm m}(1+h_0k_0+c_hk_0v_{i-1})\dot{\delta}_i+a_{\rm m}k_0\delta_i\\ &\quad=a_{\rm m}(1+c_hk_0v_{i-1})\dot{\delta}_{i-1}+a_{\rm m}k_0\delta_{i-1}\end{aligned} \quad (36)$$

and the transfer function becomes

$$G_{\rm var}(s)=\frac{a_{\rm m}(1+c_hk_0v_{i-1})s+a_{\rm m}k_0}{s^2+a_{\rm m}(1+h_0k_0+c_hk_0v_{i-1})s+a_{\rm m}k_0}. \quad (37)$$

In the case of constant separation error gain $k\equiv k_0$, i.e., when $\sigma=0$, (35) reduces to

$$\begin{aligned}\ddot{\delta}_i =& a_{\rm m}(1+c_hk_0v_{i-1})\dot{\delta}_{i-1}+a_{\rm m}k_0\delta_{i-1}\\ &-a_{\rm m}(1+h_0k_0+c_hk_0v_{i-1})\dot{\delta}_i-a_{\rm m}k_0\delta_i\\ &+c_ha_{\rm m}^2(v_{r,i-2}+k_0\delta_{i-2}-v_{r,i-1}-k_0\delta_{i-1})v_{r,i}\\ &-c_ha_{\rm m}^2v_{r,i-1}(v_{r,i-1}+k_0\delta_{i-1})\\ &+c_ha_{\rm m}^2v_{r,i}(v_{r,i}+k_0\delta_i)\\ &-c_ha_{\rm m}k_0v_{r,i}[v_{r,i-1}-h_0a_{\rm m}(v_{r,i-1}+k_0\delta_{i-1})\\ &+c_ha_{\rm m}(v_{r,i-2}+k_0\delta_{i-2}-v_{r,i-1}-k_0\delta_{i-1})v_{i-1}\\ &+c_ha_{\rm m}v_{r,i-1}(v_{r,i-1}+k_0\delta_{i-1})]\\ &+2c_ha_{\rm m}k_0v_{r,i}[v_{r,i}-h_0a_{\rm m}(v_{r,i}+k_0\delta_i)\\ &+c_ha_{\rm m}(v_{r,i-1}+k_0\delta_{i-1}-v_{r,i}-k_0\delta_i)v_i\\ &+c_ha_{\rm m}v_{r,i}(v_{r,i}+k_0\delta_i)]+c_ha_{\rm m}^2\\ &\cdot(v_{r,i-1}+k_0\delta_{i-1}-v_{r,i}-k_0\delta_i)(3v_{r,i}+2k_0\delta_i) \end{aligned} \quad (38)$$

which after linearization leads to the same transfer function (37). It is now straightforward to show that $G_{\rm var}(s)$ given by (37) satisfies the magnitude requirement $|G_{\rm var}(j\omega)<1\;\forall\,\omega>0$ if and only if

$$k_0>\frac{2(1-a_{\rm m}h_0)}{a_{\rm m}h_0(h_0+2c_hv_{i-1})}. \quad (39)$$

To compare this string stability condition with the one obtained in [3] and [5] for the case where both h and k are constant, we set $c_h=0$ in (37) to obtain

$$G(s)=\frac{a_{\rm m}s+a_{\rm m}k_0}{s^2+a_{\rm m}(1+h_0k_0)s+a_{\rm m}k_0}. \quad (40)$$

This is the same transfer function obtained in [5], where it is shown that the corresponding string stability condition is

$$k_0>\frac{2(1-a_{\rm m}h_0)}{a_{\rm m}h_0^2}. \quad (41)$$

The comparison of (39) to (41) reveals that string stability is easier to achieve in the variable h case than in the fixed h case, due to the additional term $2c_hv_{i-1}$ in the denominator of (39). Indeed, the Bode plots of $G(s)$ and $G_{\rm var}(s)$ presented in Fig. 10 show that the variable time headway reduces the magnitude peak of the transfer function. The price paid for this reduction is that $|G_{\rm var}(j\omega)|$ does not drop as fast as $|G(j\omega)|$ at higher frequencies. However, this is a good tradeoff. Since the natural dynamics of a CHV platoon act as a low-pass filter due to the low actuation-to-weight ratio, frequencies above 0.4 Hz are much less important than frequencies up to 0.4 Hz.

Finally, we should note that it is tedious, but straightforward to extend all of the above analysis to the case $q_{\rm m}>0$, since the linearization process eliminates the quadratic term and its derivatives. Therefore, the same conclusions drawn for the PI controller remain valid for the PIQ controller with variables h and k.

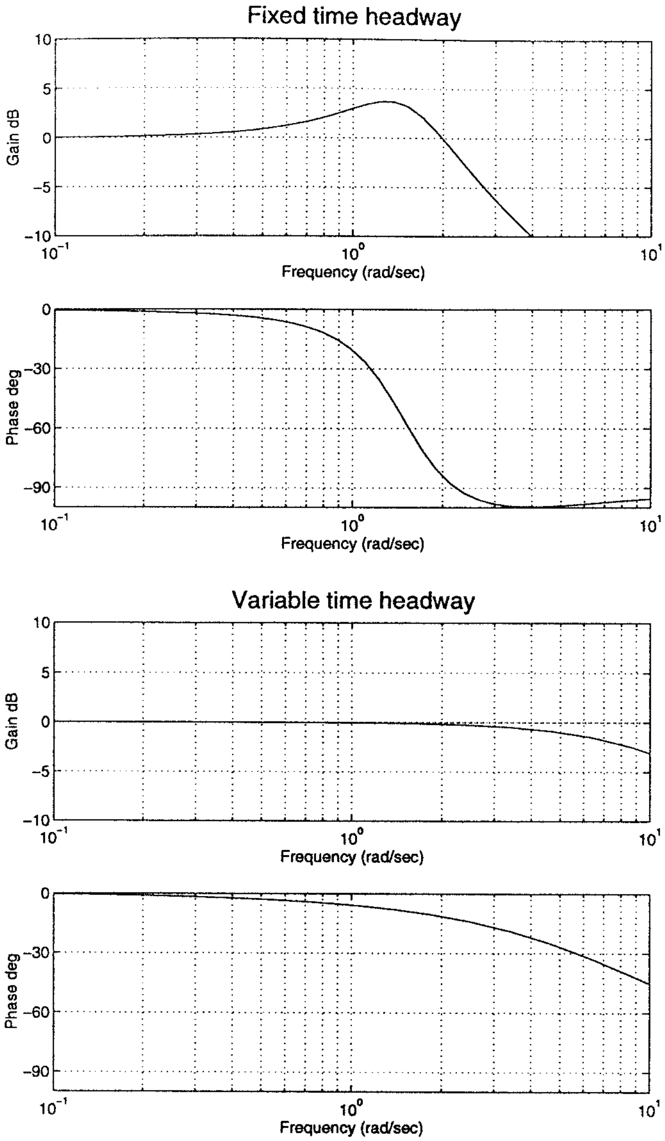

Fig. 10. Typical Bode plots of $G(s)$ and $G_{\mathrm{var}}(s)$.

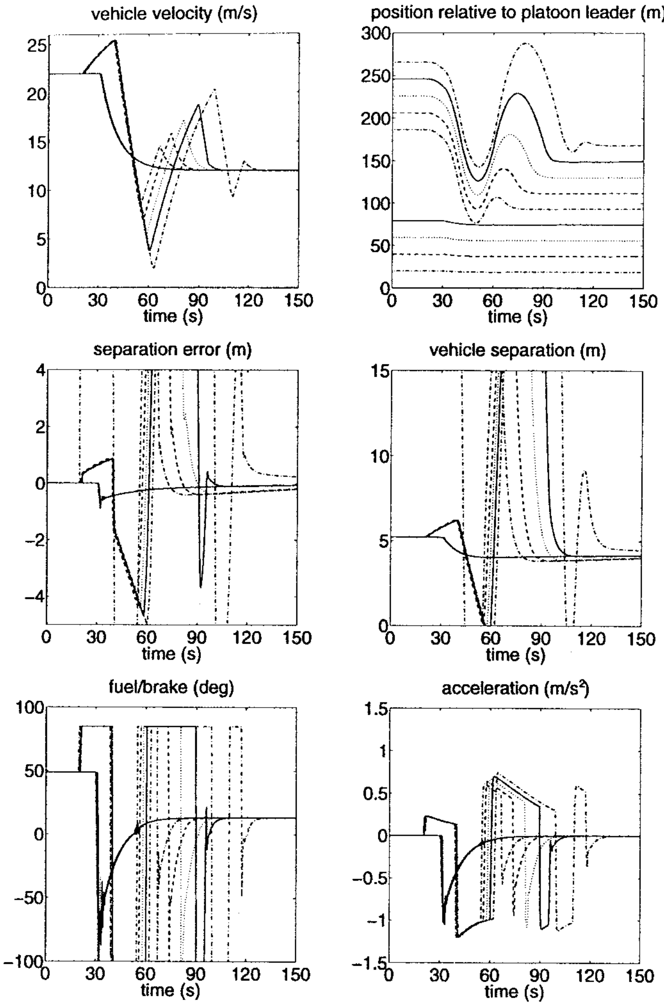

Fig. 11. Merge and brake maneuver, $h = \mathrm{sat}(0.1 - 0.2v_r)$.

IV. Merge Maneuvers

The nonlinear spacing policies presented in the previous section have been designed to improve platoon performance and control smoothness during autonomous operation, i.e., in the absence of intervehicle communication. Since the focus was on the string stability properties of our controllers, we only considered a *single-platoon* scenario for our simulations. The basic advantage of the platoon structure is that its small intervehicle spacings guarantee that even if there are collisions, they will occur at small relative velocity and thus will not be damaging. Things are much more complicated, however, when two platoons initially separated by a large distance merge to form a single platoon: the risk of collisions at high relative speed is significantly increased. Hence, a considerable amount of research effort is currently being devoted to developing robust and safe strategies for merging and splitting platoons. The most challenging scenario in this case is a merge/brake maneuver: after the merge maneuver has started and the following platoon has accelerated, the lead platoon decelerates hard.

It is then natural to ask whether the controllers developed in the previous section preserve their performance characteristics in merge/brake scenarios. This becomes then an issue of *robustness* with respect to a larger class of commanded maneuvers. To investigate whether our adaptive nonlinear controllers featuring variable time headway and/or variable separation error gain are robust enough to safely handle merge commands, we simulate their response under a challenging *merge-and-brake* maneuver: first, a five-vehicle platoon is given a step command at $t = 20$ s to merge with a similar formation initially 87.75 m ahead. The leading platoon maintains a constant speed of 22 m/s. Then, 10 s after the merge has started, the leading platoon abruptly decreases its speed from 22 to 12 m/s. The information available to the leader of the following platoon consists only of its relative position and velocity with respect to the last vehicle of the preceding platoon. The results obtained using variables h or k spacing policy are shown in Figs. 11 and 12, respectively. Fig. 13 illustrates the response of the controller used in Fig. 9, which combines the two terms with $\sigma = 0.1$.

Comparing Figs. 11 and 13, we see that the two controllers which behaved almost identically in the simpler

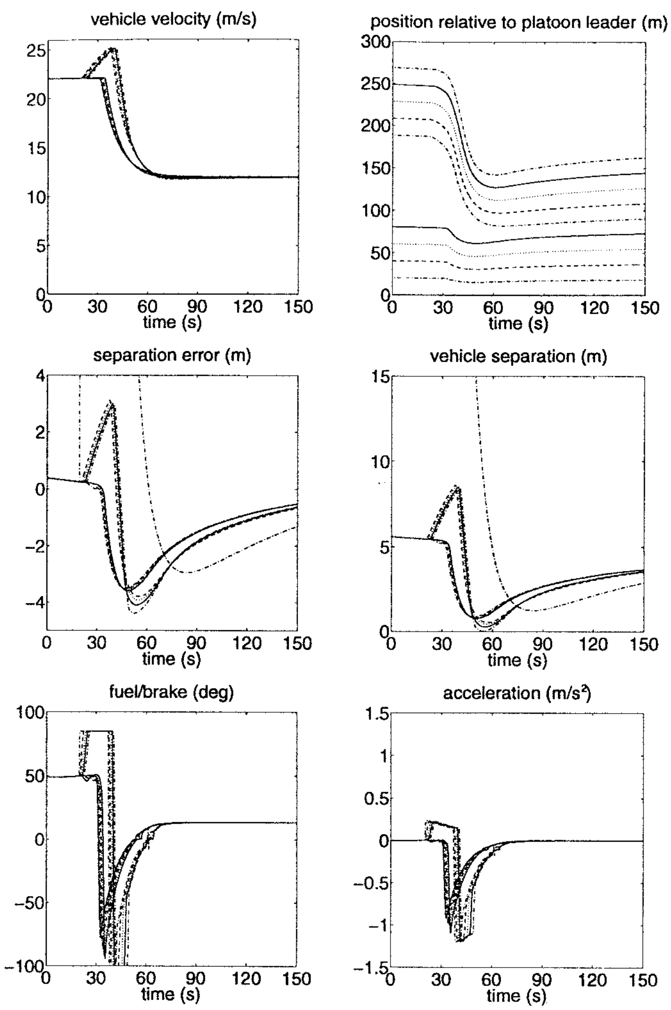

Fig. 12. Merge and brake maneuver, variable k, $\sigma = 50$.

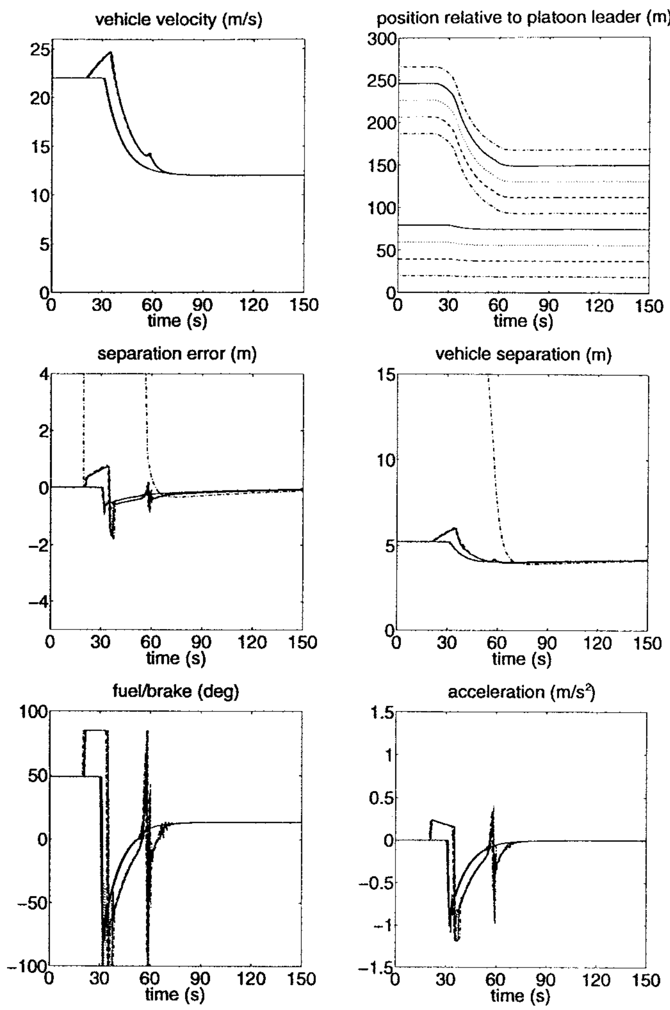

Fig. 13. Merge and brake maneuver, $h = \mathrm{sat}(0.1 - 0.2v_r)$, variable k, $\sigma = 0.1$.

deceleration/acceleration maneuver shown in Figs. 5 and 9 are anything but identical under this much more demanding merge/brake maneuver. In sharp contrast to the large errors and multiple collisions observed in Fig. 11 where only variable h is used, the addition of a seemingly mild nonlinearity in the separation error gain yields a nearly ideal response in Fig. 13. In reality, of course, this nonlinearity is not mild. As discussed in Section II-E, the benefits of variable separation error gain become significant as separation errors become large, which is certainly the case in this merge/brake scenario right after the merge command is issued. The role of the variable separation error gain for improving the robustness of the controller is further illustrated by comparing Figs. 7 and 12: the performance of the variable k controller is quite consistent under the two different scenarios. On the other hand, the variable h term alone does not provide enough robustness, as is evident from Figs. 5 and 11. Clearly, the added complexity of the variable separation error gain should be viewed as necessary for maneuvers involving more than one platoon.

V. Qualitative Comparison

According to the AHS precursor systems analysis for commercial vehicles and transit [1], longitudinal control of truck platoons will be one of the most challenging problems for commercial AHS. The control schemes examined here are promising, but need to be tested in real experiments. Before that, however, their advantages and disadvantages must be clearly understood. Each of the above modifications adds some complexity to the control algorithm, making it more computationally demanding, but at the same time results in improved performance. Comparing all the presented simulation results is not enough to determine which modifications are worth implementing and which are not, since these simulations are by no means exhaustive. Furthermore, each modification has something different to offer, and no single criterion can be used to compare and rank them. Therefore, we have compiled two qualitative comparison charts, which are based on our analytic results and on our extensive simulations of several AHS scenarios. In the diagrams of Figs. 14 and 15, each circle represents a different controller configuration. All configurations consist of a proportional and an integral term with adaptive gain and in addition may feature a Q term (denoted by `q`), variable time headway (denoted by `h`), or variable separation error gain (denoted by `k`).

We start with the results presented in Section III. The two criteria selected for this comparison are the two most important

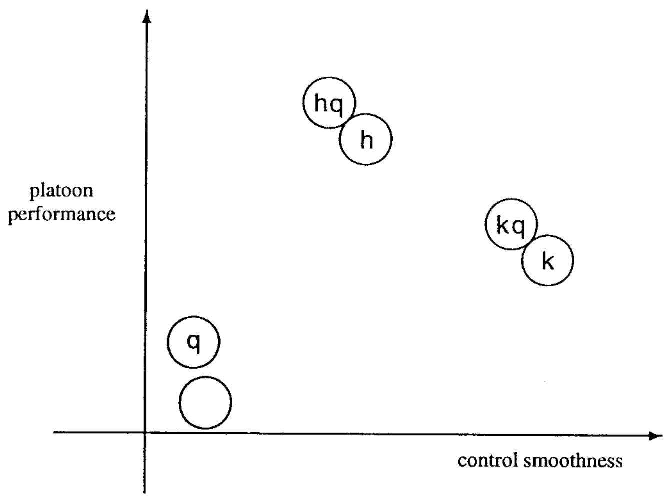

Fig. 14. Qualitative comparison chart of CHV longitudinal control schemes (autonomous operation).

ones from the AHS point of view: *control smoothness*, which is directly related to fuel efficiency and driver comfort, and *platoon performance*, which is related to safety and traffic throughput. Control schemes are considered to exhibit better platoon performance if they render the string stability property easier to achieve and if they result in errors which are smaller in magnitude. Fig. 14 should be used as a "visual aid" in determining the most appropriate longitudinal control scheme for a CHV platoon. Each choice involves a tradeoff between control smoothness, platoon performance, and controller complexity. In autonomous operation, for example, it is always worth using either variable time headway or variable separation error gain. With either of these modifications, both control smoothness and platoon performance are much better than without any of the two, and this benefit justifies the additional control complexity. If platoon performance is the primary consideration, then variable time headway is the modification of choice, while variable separation error gain should be preferred when control smoothness is more important. It is also clear that if any of these two is used, the additional complexity of a nonlinear Q term may not be justified, since the resulting change is barely noticeable.

The situation changes if we consider *robustness* with respect to a large variety of scenarios as a third criterion in addition to control smoothness and platoon performance. If we expect our controller to perform safely even when faced with abrupt merge commands followed by significant decelerations of the lead platoon, without relying on the usually considered additional layer of "nonlinear path planning," then we must use the three-dimensional (3-D) diagram of Fig. 15. The conclusion that it is always worth using either variable time headway or variable separation error gain is still valid. However, the variable separation error gain contributes much more to the robustness of the controller. Now it becomes clear that even when platoon performance is more important than control smoothness, it is advisable to tolerate the additional complexity of a variable k term with a small value of σ, since that yields a very significant robustness enhancement to merge maneuvers. Again, when either variable h or k

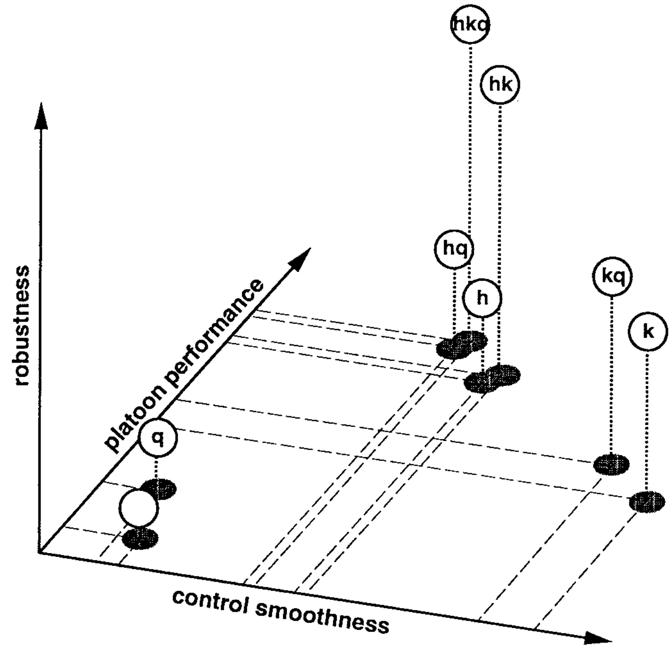

Fig. 15. A more elaborate qualitative comparison.

is used, the additional complexity of a nonlinear Q term may not be justified, since the resulting change is barely noticeable. Taking into consideration all of the above, the scheme which utilizes both variable h and variable k with $\sigma = 0.1$ appears to have the clear advantage over all other autonomous controllers.

ACKNOWLEDGMENT

The contents of this paper reflect the views of the authors who are responsible for the facts and the accuracy of the data presented herein. The contents do not necessarily reflect the official views or policies of the State of California. This paper does not constitute a standard, specification, or regulation.

REFERENCES

[1] F. Bottiger, H. D. Chemnitz, J. Doorman, U. Franke, T. Zimmermann, and Z. Zomotor, "Commercial vehicle and transit AHS analysis," *Precursor Systems Analyzes of Automated Highway Systems,* Federal Highway Administration, Rep. FHWA-RD-95-XXX, 1995.

[2] C. Chien and P. Ioannou, "Automatic vehicle following," in *Proc. 1992 American Control Conf.,* Chicago, IL, pp. 1748–1752.

[3] W. L. Garrard, R. J. Caudill, A. L. Kornhauser, D. MacKinnon, and S. J. Brown, "State-of-the-art of longitudinal control of automated guideway transit vehicles," *High Speed Ground Transportation J.,* vol. 12, pp. 35–68, 1978.

[4] J. K. Hedrick, D. H. McMahon, V. K. Narendran, and D. Swaroop, "Longitudinal vehicle controller design for IVHS systems," in *Proc. 1991 American Control Conf.,* Boston, MA, pp. 3107–3112.

[5] P. Ioannou and Z. Xu, "Throttle and brake control systems for automatic vehicle following," *IVHS J.,* vol. 1, pp. 345–377, 1994.

[6] S. Sheikholeslam and C. A. Desoer, "Longitudinal control of a platoon of vehicles," in *Proc. 1990 American Control Conf.,* San Diego, CA, pp. 291–297.

[7] S. E. Shladover, "Longitudinal control of automated guideway transit vehicles within platoons," *ASME J. Dynamic Syst., Meas., Contr.,* vol. 100, pp. 302–310, 1978.

[8] P. Varaiya, "Smart cars on smart roads: Problems of control," *IEEE Trans. Automat. Contr.,* vol. 38, pp. 195–207, 1993.

[9] Z. Xu and P. Ioannou, "Adaptive throttle control for speed tracking," *Vehicle System Dynamics,* vol. 23, pp. 293–306, 1994.

[10] D. Yanakiev and I. Kanellakopoulos, "Longitudinal control of heavy-duty vehicles for automated highway systems," in *Proc. 1995 American Control Conf.,* Seattle, WA, pp. 3096–3100.

[11] ——, "Variable time headway for string stability of automated heavy-duty vehicles," in *Proc. 34th IEEE Conf. Decision and Control,* New Orleans, LA, Dec. 1995, pp. 4077–4081.

[12] ——, "Speed tracking and vehicle follower control design for heavy-duty vehicles," *Vehicle System Dynamics,* vol. 25, pp. 251–276, 1996.

Diana Yanakiev (S'94–M'98) was born in Rousse, Bulgaria, in 1965. She received the Diploma from the Technical University of Sofia, Bulgaria, in 1989 and the M.S. and Ph.D. degrees from the University of California, Los Angeles, in 1994 and 1997, respectively, all in electrical engineering.

Since September 1997, she has been a Senior Engineer with Cummins Engine Company, Inc., Columbus, IN. Her research interests are in nonlinear control, especially as applied to engine control and automation of commercial heavy-duty vehicles.

Ioannis Kanellakopoulos (S'86–M'91) was born in Athens, Greece, in 1964. He received the Diploma in electrical engineering from the National Technical University of Athens, Athens, in 1987 and the M.S. and Ph.D. degrees in electrical engineering from the University of Illinois, Urbana-Champaign, in 1989 and 1992.

Since July 1992, he has been with the Department of Electrical Engineering, University of California, Los Angeles, where he is currently an Associate Professor. His research interests include adaptive and nonlinear control theory with applications to advanced vehicle control systems, intelligent transportation systems, autonomous vehicles, and electric motors.

Dr. Kanellakopoulos was the recipient of the 1993 George S. Axelby Outstanding Paper Award of the IEEE TRANSACTIONS ON AUTOMATIC CONTROL, a 1993 NSF Research Initiation Award, a 1995 NSF CAREER Award, the 1996 AlliedSignal Faculty Research Award from the UCLA School of Engineering and Applied Science, a 1997 Eta Kappa Nu Outstanding Young Electrical Engineer Honorable Mention, and the 1998 Donald P. Eckman Award of the American Automatic Control Council.